Nanotechnology **20** (2009) 365302 (7pp) doi:10.1088/0957-4484/20/36/365302

DNA-templated synthesis of ZnO thin layers and nanowires

Petia Atanasova[1,4], R Thomas Weitz[2], Peter Gerstel[1], Vesna Srot[3], Peter Kopold[3], Peter A van Aken[3], Marko Burghard[2] and Joachim Bill[1]

[1] Institut für Materialwissenschaft, Universität Stuttgart and Max-Planck-Institut für Metallforschung, Heisenbergstraße 3, 70569 Stuttgart, Germany
[2] Max-Planck-Institut für Festkörperforschung, Heisenbergstraße 1, 70569 Stuttgart, Germany
[3] Stuttgart Center for Electron Microscopy, Max-Planck-Institut für Metallforschung, Heisenbergstraße 3, 70569 Stuttgart, Germany

E-mail: atanasova@mf.mpg.de

Received 8 May 2009, in final form 29 July 2009
Published 18 August 2009
Online at stacks.iop.org/Nano/20/365302

Abstract
In this paper, we report a novel synthetic approach towards electrically conductive ZnO nanowires close to ambient conditions using λ-DNA as a template. Initially, the suitability of DNA to assemble ZnO nanocrystals into thin coatings was investigated. The ZnO nanowires formed on stretched and aligned λ-DNA molecules were prepared via chemical bath deposition (CBD) of zinc acetate in methanol solution in the presence of polyvinylpyrrolidone (PVP). After 10 deposition cycles, the nanowires exceed 10 μm in length and the height can be varied from 12 to around 40 nm. The nanocrystalline structure of the ZnO wires was confirmed by high-resolution transmission electron microscopy (HRTEM). The electrical conductivity was found to be of the order of several Ω cm at room temperature in two terminal measurements.

S Supplementary data are available from stacks.iop.org/Nano/20/365302

1. Introduction

The development of novel functional nano-sized materials as components for electronic devices is a challenging task, since the conventional techniques (e.g. microcontact printing, electron-beam lithography and photolithography) face resolution problems with the formation of well-defined 1D and 2D nanostructures. Therefore, considerable attention has been devoted to 'bottom–up' methods, where molecular components self-assemble into more complex architectures. Nature provides a wide range of biomacromolecules (e.g. proteins, peptides, amino and nucleic acids), which can serve as templates, scaffolds and stabilizers in the formation of new hybrid organic–inorganic nanostructures with a specific shape and unique properties [1–3]. A particularly attractive biological template is the double helix of DNA possessing a linear structure, mechanical rigidity, as well as physicochemical stability. In the past decade, DNA has been extensively used for controlled arrangement of molecules and nanoparticles into nanowires. For instance, low conductive DNA [4] was successfully used as a template for the formation of conductive nanowires composed of different materials such as metals (Pd [5–7], Pt [8], Au [9], Ag [10, 11], Cu [12] and Co [13]), nanoparticles [14], conducting polymers [15, 16], and semiconductors like CdS [17, 18], PbS [19], CuS [20] and ZnS [21].

In particular, semiconducting nanowires are of interest for the fabrication of functional electronic devices. Individual ZnO nanowires have been used as active channels in field effect transistors [22, 23], as well as in gas sensors and UV detectors [24–26]. Different chemical, electrochemical and physical deposition techniques have been applied to create highly oriented arrays of ZnO nanorods and nanowires of various diameters and lengths [27–29]. A promising novel synthesis approach towards ZnO nanowires with tuneable structure is the mineralization of ZnO onto aligned biomacromolecule scaffolds.

Herein, we describe a route for the synthesis of electrically conductive ZnO nanowires templated on λ-DNA strands onto electrically relevant substrates. CBD was applied to

[4] Author to whom any correspondence should be addressed.

mineralize ZnO along the DNA, using zinc acetate dihydrate as a precursor. The ZnO nanowires were characterized by analytical and microscopy methods. The electrical conductivity was confirmed by current–voltage measurements.

2. Experimental details

2.1. Chemicals and materials

Double stranded λ-DNA (48 502 bp in length) from BioLabs was used in the experiments. $Zn(OOCCH_3)_2{\cdot}2H_2O$ (puriss pa, Fluka), PVP (PVP10, $M = 10\,000$, Sigma-Aldrich), TEAOH (purum, Fluka, ∼25% in methanol) and methanol (VLSI Selectipur, BASF) were used without further purification. The aqueous solutions were prepared with deionized water (MilliQ) (Millipore, 18.2 MΩ). The cleaning procedure for Si-wafers (100) (1×1) cm^2 was done by consecutive ultrasonification in MilliQ water and a mixture of 1:1 acetone:ethanol for 10 min, plasma cleaning for 10 min, and finally ultrasonification in MilliQ water for 10 min. The root mean-square roughness determined by AFM of the surface was 0.2 nm from (5×5) μm^2 area. All reaction vessels were dried in an oven for 24 h at 150 °C prior to use.

2.2. General procedure for mineralization of ZnO on DNA

DNA immobilization. The adhesion between the negatively charged DNA and the substrate can be facilitated by the presence of divalent cations. Therefore, all DNA solutions were prepared by dilution of a stock DNA solution (500 μg ml^{-1}) with aqueous zinc acetate solution (0.45 mM). The latter were heated at 65 °C for 10 min and cooled down in ice prior to use. For the immobilization of a DNA template layer, a droplet of λ-DNA (40 μg ml^{-1}) was allowed to evaporate on a silicon wafer at room temperature. The stretching and alignment of the DNA molecules was done as follows: 5 μl λ-DNA (20 μg ml^{-1}) was spotted onto the substrate surface and allowed to incubate for 30 s at room temperature. The droplet was blown in one direction by a stream of nitrogen gas applied at an angle of ∼45° to the normal to the substrate surface for several minutes.

Deposition solution and mineralization. The deposition solution preparation is described in details elsewhere [30]. Briefly, stock methanol solutions of zinc acetate (40 mmol l^{-1}), TEAOH (100 mmol l^{-1}) and PVP (20 mmol l^{-1}) were prepared and could be used for several days. The precursor solution with ratio of [PVP]:[Zn^{2+}] = 1:1 and final concentrations [Zn^{2+}] = 10 mM, [PVP] = 10 mM, and [TEAOH] ∼ 25 mM was prepared by mixing one volume unit of the zinc acetate with two volume units of PVP stock solutions. Then, one volume unit of TEAOH stock solution was added dropwise using a peristaltic pump at a flow rate of 1.04 ml min^{-1} under continuous stirring. The prepared solution is good for use up to 24 h. Immediately following the alignment or the droplet evaporation, respectively, a substrate with the immobilized DNA molecules was placed in one aliquot of the precursor solution, closed in a well dried vessel and heated in an oil bath at 60 °C for 1.5 h. Subsequently, the substrate was gently rinsed with methanol and dried with argon. Using the procedure described above, the mineralization reaction was repeated 10 times (10 cycles).

2.3. Sample characterization

Atomic force microscopy (AFM) imaging was performed on a Digital Instruments Nanoscope III applying the tapping mode with silicon cantilevers and a super sharp tip (TESP-SS).

Scanning electron microscopy (SEM) was done using a JEOL JSM-6300F (JEOL Ltd, Tokyo, Japan) operating at an accelerating voltage of 3 kV. The images were recorded using a secondary electron (SE) detector.

A transmission electron microscopy (TEM) specimen was prepared using the conventional cross-section method. Unidirectional ion milling from the substrate to the ZnO nanowires was performed using an ion milling and polishing system at 3.5 keV (Model 1010, EA Fischione Instruments Inc., Export, USA). Final polishing was performed at 0.5 keV. During the ion milling process, the specimen was cooled with liquid nitrogen.

HRTEM was performed using a JEOL JEM 4000 FX (JEOL Ltd, Tokyo, Japan) operated at 400 kV.

Analytical TEM studies were carried out in a VG HB501UX dedicated scanning transmission electron microscope (STEM) operating in an ultra-high vacuum at an accelerating voltage of 100 kV. The beam diameter was 0.7 nm (full width at half maximum (FWHM)). This microscope has a cold field emission source and is equipped with an energy-dispersive (EDX) x-ray spectrometer (Noran System SIX, Thermo Fischer Scientific, Waltham, USA) and an electron energy-loss spectrometer (EELS) (Gatan UHV Enfina system, Gatan Inc., Pleasanton, USA). For the acquisition of EELS, spectra dispersions of 0.1 and 0.3 eV/channel were used.

Photoluminescence measurements were performed with a spectrofluorometer—Spex FluoroLog 3, Horiba Jobin Yvon.

2.4. Preparation of the sample for electrical measurements

ZnO nanowires were synthesized directly onto silicon dioxide covered degenerately doped silicon wafers, onto which gold–palladium alignment marks had been predefined. The ZnO nanowires were located by AFM relative to these alignment marks and contacted by electron-beam lithography. A standard double layer PMMA resist (200 k, 7 wt% and 950 k, 5 wt%) was used. After lift-off, the substrates were treated with an argon plasma for 3 min and 80 nm of aluminium was deposited without breaking the vacuum. The metal was removed by standard lift-off in *N*-methyl-2-pyrrolidone. Electrical measurements were performed at room temperature in ambient atmosphere.

3. Results and discussions

3.1. Formation of DNA-based nanocrystalline ZnO thin layers and nanowires

Firstly, we investigated the suitability of DNA as a carrier of surface charges to assemble ZnO nanocrystals into a thin layer. The interaction between the polar ZnO nanoparticles and

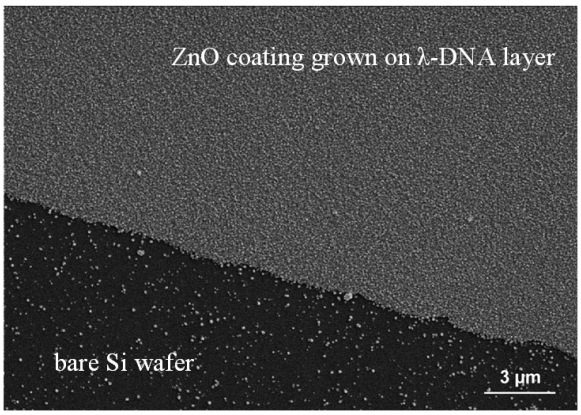

Figure 1. SEM image (SE) of ZnO film on λ-DNA after 10 deposition cycles on the silicon substrate.

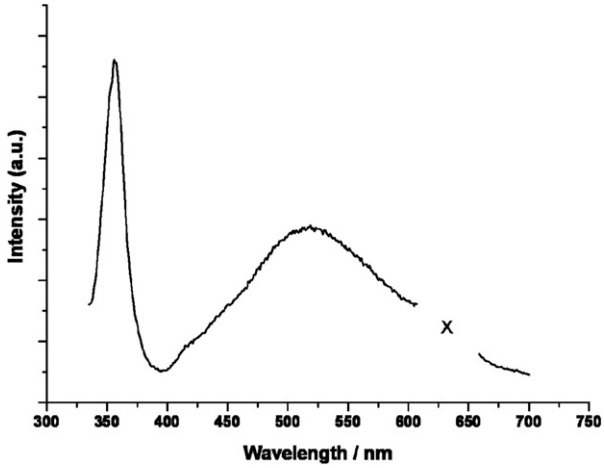

Figure 2. Photoluminescence spectrum of a ZnO/DNA film prepared by applying 20 deposition cycles. The emission was measured for excitation at 315 nm. The truncated peak (x) is the second harmonic of the excitation beam.

a sulfonate-functionalized self-assembled monolayer (SAM), resulting in the formation of thin coatings, was recently reported by Lipowski *et al* [30]. Instead of sulfonate-SAM, a silicon substrate covered with a template layer of immobilized DNA molecules was prepared and mineralized according to the procedure described in section 2. A thin uniform ZnO coating on the DNA layer is formed due to the electrostatic interaction between the polar ZnO crystallites and the negatively charged DNA molecules. The ZnO deposition on DNA is exceptionally selective. This can be seen clearly in figure 1, where two separate regions can be distinguished. The bottom one represents a bare Si-wafer substrate with isolated ZnO particles, while the upper part is a ZnO nanocrystalline layer grown onto the immobilized DNA.

After 10 deposition cycles, the roughness of the film was measured by AFM. The root mean squared deviation (rms) value of around 11 nm determined from a $(10 \times 10)\ \mu m^2$ area is slightly larger than the roughness of ZnO films formed on sulfonate-terminated SAM (rms $=$ 5 nm on a $(5 \times 5)\ \mu m^2$ area) [30].

We have performed optical spectroscopy to assess the quality of the deposited films and the size of the ZnO nanoparticles. The emission spectra (figure 2) (315 nm excitation) of the obtained ZnO films exhibit two components: a UV peak at about 356 nm and a green peak at about 518 nm. The strong UV emission peak is attributed to the ZnO band-edge emission and its intensity indicates a high crystalline quality [31]. It is generally known that the increase of the particle size causes redshift of the UV band. In contrast to bulk ZnO, in which the band gap is 3.377 eV (367 nm) [32], the energy of UV emission in figure 2 is shifted to 3.48 eV (356 nm). Using an analytical approximation for the first excited electronic state [32] (the equation is given in supporting information available at stacks.iop.org/Nano/20/365302), we obtain a value of 5.4 nm for the nanoparticle size. The first derivative curve of the emission spectrum is used and the point of inflection is taken as the emission edge, in order to get a more precise measure of the shift. The calculated value is in very good agreement with the value reported in the literature [33]. The second broad green peak can be attributed to oxygen vacancies at the surface of the nanocrystalline ZnO layer, where electrons in single occupied oxygen vacancies recombine with photoexcited holes in the valence band [34].

After having shown that the mineralization of ZnO on DNA in the mild conditions of CBD is possible and selective, the affinity of ZnO nanocrystals to DNA was further utilized in the formation of precise and well-defined DNA-templated one-dimensional nanostructures. For this purpose, the DNA molecules had to be separately aligned to serve as templates for the fabrication of nanowires. Their assembly was performed in two steps: (i) alignment of DNA molecules on a substrate by molecular combing [35], followed by (ii) mineralization of ZnO by CBD. In detail, the stretching process of the DNA was performed in the presence of a small amount of divalent metal ions (Zn^{2+}) that are needed to connect the negatively charged DNA helix with the hydroxyl groups on the substrate surface. For their deposition, a droplet of λ-DNA solution was incubated on a silicon substrate. Then, a stream of nitrogen gas was applied at an angle of ∼45° to the normal of the surface [36]. The alignment of the DNA by the nitrogen stream was confirmed by AFM. The mineralization of the ZnO was then performed by placing the substrate horizontally in the deposition solution and subsequently heated at 60 °C for 1.5 h.

In contrast to water-containing deposition solutions, where the hydrolysis of zinc salts cannot be easily controlled and DNA molecules are easily soluble, methanol used as a solvent has the advantage of keeping an anhydrous environment and does not allow desorption of the fixed DNA molecules from the substrate surface during the mineralization process. Furthermore, the addition of PVP to the deposition solution restricts the crystal growth of ZnO, and thus crystallites in the wurtzite form with a diameter of only few nanometres are formed [37]. Initially, heterogeneous aggregation of these particles on the substrate is favoured over the homogeneous aggregation in the solution [38]. Hence, owing to the polar surface of ZnO, the crystallites formed in solution may attach with a preferred orientation to the negatively charged backbone of DNA and assemble along the strands. However, after 1.5 h

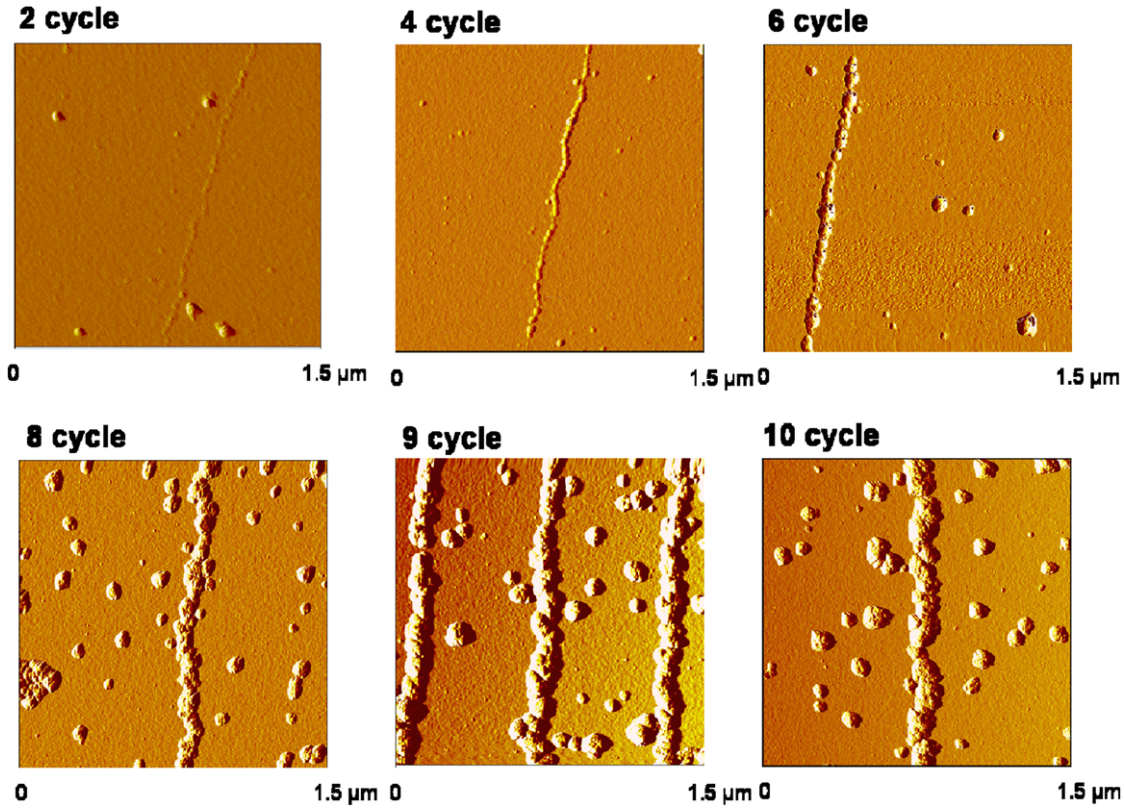

Figure 3. AFM amplitude images of DNA-templated ZnO nanowires on silicon substrates. The nanowire thickness increases with the number of deposition cycles.

(This figure is in colour only in the electronic version)

the competitive aggregation in solution starts to dominate, and the particle diameter grows continuously with time [30]. Therefore, in order to avoid attachment of bigger particles, and thus to increase the roughness of the structures, the substrates were removed from the reaction vessel every 1.5 h and, after gentle rinsing and drying, they were placed again in a fresh deposition solution. The procedure described above was repeated up to 10 times in order to obtain continuous ZnO nanowires along the DNA. AFM was used to monitor the height of the formed ZnO nanowires and to evaluate the selectivity after each deposition cycle. Control experiments in the absence of DNA were performed for comparison, where only isolated ZnO particles, but no connected ZnO wires, appear during the thermohydrolysis and grow further with each deposition cycle.

On a silicon wafer, ZnO mineralizes preferably on the aligned DNA (figure 3), while a low density of single ZnO particles was formed on the bare substrate surface. The height of the wires increases with the number of the deposition cycles up to 39.5 ± 1.8 nm (figure 4). The first few deposition cycles led only to the formation of single ZnO beads on the DNA chains. However, the appearance of ZnO crystallites on the DNA template seems to promote further deposition, and after the fourth cycle, the height of the wires increases faster.

An SEM image of ZnO nanowires after 10 deposition cycles (figure 5) confirmed the selectivity of ZnO deposition on the DNA strands and gives a view on a larger surface area.

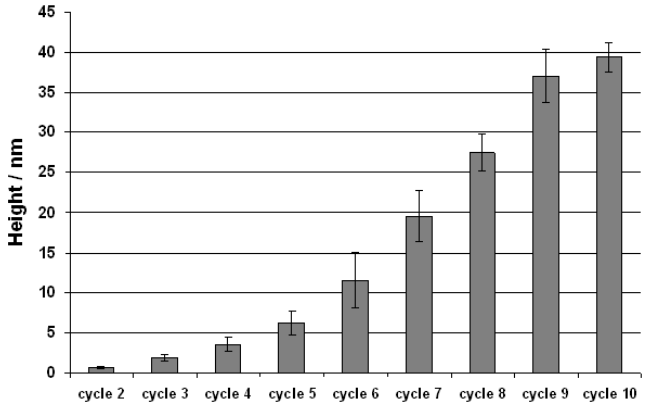

Figure 4. Average height of the ZnO/DNA nanowires on the Si-wafer substrate determined by AFM imaging of 10 nanowires.

The length of the wires exceeds 10 μm and remains nearly constant throughout the 10 deposition cycles. Most of the DNA chains are stretched and parallel to each other. However, some molecules can intersect together or even, in some isolated cases in spite of the short incubation time, fix strongly to the surface and prevent their alignment (figure 5, bottom left).

In an attempt to obtain thinner ZnO nanowires and to minimize the parasitic mineralization on the substrate surface, silicon wafers with immobilized DNA were immersed either vertically, or at an angle of ∼45°, into the deposition solution.

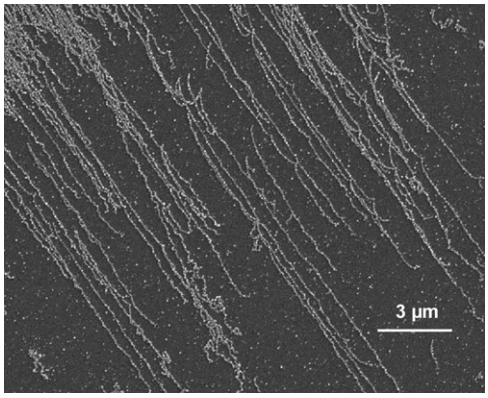

Figure 5. SEM image (SE) of aligned ZnO/DNA wires obtained after 10 deposition cycles. Most of the DNA molecules are stretched and parallel to each other.

Even though the mineralization on the bare substrate could not be avoided, the size of the ZnO particles was much smaller. As a consequence, the nanowires grow slower in height as expected and consist of smaller particles confirmed by AFM. The wire diameter was found to be significantly reduced; after 10 cycles, the height of the wires dropped from 40 nm, for a horizontal orientation of the substrate, to around 14 nm, when the substrate is tilted to about 45°. The height even drops further to around 12 nm when the substrate is vertically oriented.

3.2. Characterization of the ZnO nanowires

HRTEM images of a cross-sectional specimen of ZnO/DNA nanowire on a Si substrate were recorded (figures 6(a) and (b)) to investigate the crystalline quality of the wires and the size and orientation of the crystals. The higher magnification image (figure 6(b)) reveals the polycrystalline structure of the ZnO wires. The size of the crystals is up to 10 nm, which correlates well with the particle size calculated from the emission spectrum of the ZnO layer (see figure 2). There is no indication for texture and a certain orientation of the nanocrystals; this can be expected because the negative phosphate groups of the immobilized DNAs are uniformly distributed along the strands pointing in all directions towards the deposition solution. The ZnO nanoparticles formed in the solution are attracted approaching the helix from different directions and self-assemble statistically. The height of the wires evaluated from the micrographs is in accordance with the values extracted from the AFM measurements described above.

Analytical TEM (EDX and EELS) experiments were performed in different regions of the ZnO nanowires. The EDX spectrum (supporting information available at stacks.iop.org/Nano/20/365302) confirmed the presence of Zn and O belonging to the ZnO nanowires. The ZnO reference spectra [39] and the experimental EELS spectra acquired on the ZnO nanowires are compared in figure 7. The experimental low-loss spectrum and the background subtracted O-K edge spectrum acquired in the energy region between 520 and 600 eV confirm the chemical identity of the ZnO nanowires with ZnO bulk material. Additionally, our experimental EELS spectra were compared to the experimental and theoretical O-K spectra published by Mizoguchi *et al* [40] which verify that the ZnO wires posses the wurtzite structure.

3.3. Electrical measurements

In order to evaluate the electrical conductivity of the ZnO wires, we have synthesized ZnO/DNA wires directly on silicon dioxide-coated silicon wafers. The wires were located by AFM relative to predefined alignment marks and contacted by standard electron-beam lithography, thermal metal deposition and lift-off. Prior to the metal deposition, a short argon plasma treatment was performed to enhance the contact between the aluminium and the ZnO nanowire. Measurable electric currents could only be detected from ZnO wires if at least 10 deposition cycles were performed. However, among the investigated wires obtained using 10 cycles, only ∼25% were found to be electrically conductive. The current–voltage characteristics of a representative conducting wire contacted with 80 nm of Al is shown in figure 8. From the wire diameter

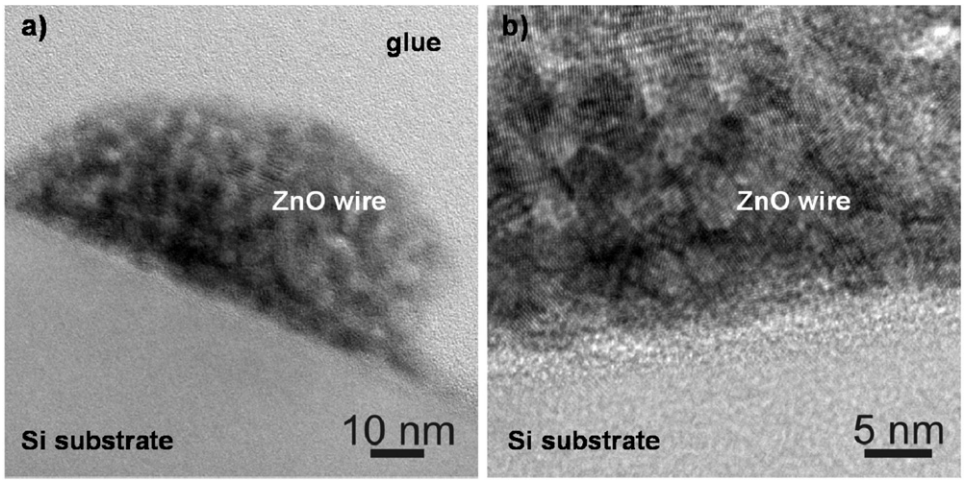

Figure 6. HRTEM images of a cross-sectional TEM specimen of a ZnO/DNA nanowire on a Si substrate ((a), (b)).

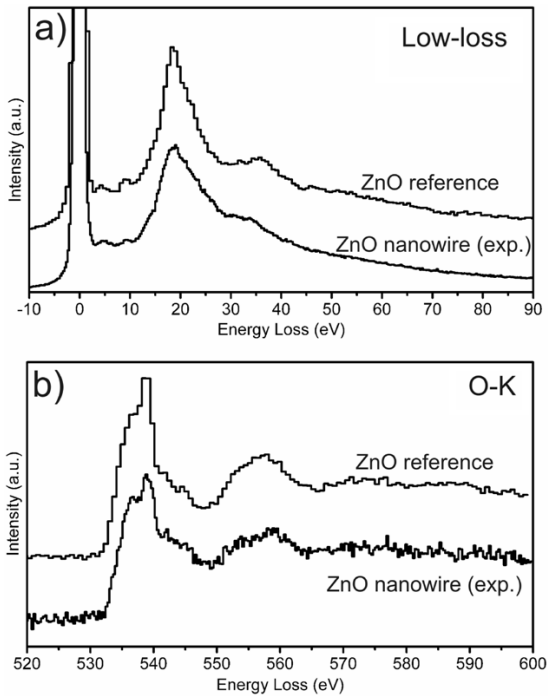

Figure 7. ZnO reference ((a), (b) top) and experimental EELS spectra recorded on the ZnO nanowire ((a), (b) bottom) acquired in the low-loss energy range (a) and in the energy range of the O-K edge (b).

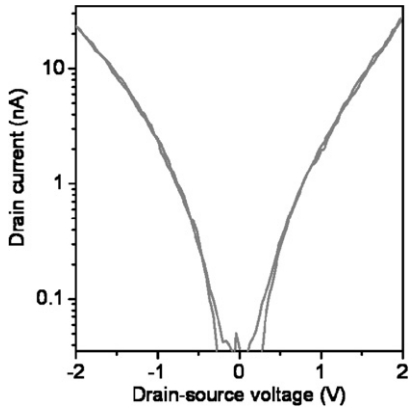

Figure 8. Current voltage characteristics of a ZnO nanowire contacted by aluminium top electrodes. The data correspond to a bias voltage cycle 0 V $\rightarrow$ +2 V $\rightarrow$ −2 V $\rightarrow$ 0 V.

of ∼40 nm and the ∼700 nm separation between the contacts, a resistivity of ∼18 Ω cm is estimated at a bias voltage of 2 V (neglecting contact resistance).

A similarly high resistivity has been reported for ZnO nanowires grown by vapour phase deposition [41]. It demonstrates that a better connectivity between the ZnO grains in the wires is needed in order to enhance the wires' electrical performance.

4. Summary and conclusions

We have developed a novel method for fabrication of ZnO nanowires in the mild conditions of CBD using λ-DNA as a scaffold. Continuous ZnO nanowires of about 10 μm in length, and with a height of ∼40 nm, were obtained in 10 deposition cycles. It was shown that the height of the wires can be reduced to 12 nm by changing the orientation of the substrate in the deposition solution. HRTEM investigations demonstrated the polycrystalline structure of the wires. Finally, electrical conductivity measurements revealed that the ZnO nanowires obtained using this method after 10 deposition cycles are electrically conductive.

Acknowledgments

The financial support of the KSB Foundation (Germany) is gratefully acknowledged. The authors thank Sabine Kühnemann for recording the SEM images, and Bernhard Fenk and Marion Kelsch for TEM specimen preparation.

References

[1] Scheibel T, Parthasarathy R, Sawicki G, Lin X M, Jaeger H and Lindquist S L 2003 *Proc. Natl Acad. Sci. USA* **100** 4527
[2] Gerstel P, Hoffmann R C, Lipowsky P, Jeurgens L P H, Bill J and Aldinger F 2006 *Chem. Mater.* **18** 179
[3] Hinds S, Taft B J, Levina L, Sukhovatkin V, Dooley C J, Roy M D, MacNeil D D, Sargent E H and Kelley S O 2006 *J. Am. Chem. Soc.* **128** 64
[4] Eley D D and Leslie R B 1963 *Nature* **197** 898
[5] Deng Z and Mao C 2003 *Nano Lett.* **3** 1545
[6] Lund J, Dong J, Deng Z, Mao C and Parviz B A 2006 *Nanotechnology* **17** 2752
[7] Nguyen K, Monteverde M, Filoramo A, Goux-Capes L, Lyonnais S, Legou P, Viel P, Goffman M and Bourgoin J P 2008 *Adv. Mater.* **20** 1099
[8] Mertig M, Ciacchi L C, Seidel R and Pompe W 2002 *Nano Lett.* **2** 841
[9] Keren A, Krueger M, Gilad R, Ben-Yoseph G, Sivan U and Braun E 2002 *Science* **297** 72
[10] Braun E, Eichen Y, Sivan U and Ben-Yoseph G 1998 *Nature* **391** 775
[11] Keren K, Berman R S and Braun E 2004 *Nano Lett.* **4** 323
[12] Monson C F and Woolley A T 2003 *Nano Lett.* **3** 359
[13] Gu Q, Cheng C and Haynie D T 2005 *Nanotechnology* **16** 1358
[14] Kinsella J M and Ivanisevic A 2007 *Langmuir* **23** 3886
[15] Dong L, Hollis T, Fishwick S, Connolly B A, Wright N G, Horrocks B R and Houlton A 2007 *Chem. Eur. J.* **13** 822
[16] Nickels P, Dittmera W U, Beyer S, Kotthaus J P and Simmel F C 2004 *Nanotechnology* **15** 1524
[17] Dong L, Hollis T, Connolly B A, Wright N G, Horrocks B R and Houlton A 2007 *Adv. Mater.* **19** 1748
[18] Kundu S and Liang H 2008 *Adv. Mater.* **20** 826
[19] Levina L, Sukhovatkin V, Musikhin S, Cauchi S, Nisman R, Bazett-Jones D P and Sargent E H 2005 *Adv. Mater.* **17** 1854
[20] Dittmera W U and Simmel F C 2004 *Appl. Phys. Lett.* **85** 633
[21] Stsiapura V, Sukhanova A, Baranov A, Artemyev M, Kulakovich O, Oleinikov V, Pluot M, Cohen J H M and Nabiev I 2006 *Nanotechnology* **17** 581
[22] Heo Y W, Tien L C, Kwon Y, Norton D P, Pearton S J, Kang B S and Ren F 2004 *Appl. Phys. Lett.* **85** 2274
[23] Cha S N, Jang J E, Choi Y, Amaratunga G A J, Ho G W, Wellang M E, Hasko D G, Kang D-J and Kim J M 2006 *Appl. Phys. Lett.* **89** 263102
[24] Law J B K and Thong J T L 2006 *Appl. Phys. Lett.* **88** 133114
[25] Wan Q, Li Q H, Chen Y J, Wang T H, He X L, Li J P and Lin C L 2004 *Appl. Phys. Lett.* **84** 3654
[26] Kind H, Yan H, Messer B, Law M and Yang P 2002 *Adv. Mater.* **14** 158
[27] Huang M H, Wu Y, Feick H, Tran N, Weber E and Yang P 2001 *Adv. Mater.* **13** 113

[28] Vayssieres L 2003 *Adv. Mater.* **15** 464
[29] Fan H L, Knez M, Scholz R, Nielsch K, Pippel E, Hesse D, Zacharias M and Guesele U 2006 *Nat. Mater.* **5** 627
[30] Lipowski P, Hoffmann R C, Welzel U, Bill J and Aldinger F 2007 *Adv. Funct. Mater.* **17** 2151
[31] Wu J J and Liu S C 2002 *J. Phys. Chem.* B **106** 9546
[32] Brus L 1986 *J. Phys. Chem.* **90** 2555
[33] Irimpan L, Nampoori V P N and Radhakrishnan P 2007 *J. Appl. Phys.* **102** 063524
[34] Vanheusden K, Warren W L, Seager C H, Tallant D R and Voigt J A 1996 *J. Appl. Phys.* **79** 7983
[35] Bensimon A, Simon A, Chiffaudel A, Croquette V, Heslot F and Bensimon D 1994 *Science* **265** 2096
[36] Li J, Bai C, Wang C, Zhu C, Lin Z, Li Q and Gao E 1998 *Nucleic Acids Res.* **26** 4785
[37] Lipowski P, Hedin N, Bill J, Hoffmann R C, Ahniyaz A, Aldinger F and Bergström L 2008 *J. Phys. Chem.* C **112** 5373
[38] Hansen P H F, Malmsten M, Bergenstahl B and Bergström L 1999 *J. Colloid Interface Sci.* **220,** 269
[39] The EELS Data Base http://www.cemes.fr/∼eelsdb/
[40] Mizoguchi T, Tanaka I, Yoshioka S, Kunisu M, Yamamoto T and Ching W Y 2004 *Phys. Rev.* B **70** 045103
[41] Schlenker E, Bakin A, Weimann T, Hinze P, Weber D H, Gölzhäuser A, Wehmann H-H and Waag A 2008 *Nanotechnology* **19** 365707